Viscoelastic Relaxation of Styrene−Butadiene Diblock Copolymer Micellar Systems. 1. Behavior in a Nonentangling, Short Polybutadiene Matrix

Hiroshi Watanabe,* Tomohiro Sato, and Kunihiro Osaki

Institute for Chemical Research, Kyoto University, Uji, Kyoto 611, Japan

Received August 24, 1995[⊗]

ABSTRACT: For blends of styrene−butadiene (SB) diblock copolymers in a nonentangling homopolybutadiene (hB) matrix, viscoelastic data obtained in a previous study (Watanabe, H.; Kotaka, T. *Macromolecules* **1983**, *16*, 769) were reexamined to elucidate features of relaxation of *individual* B blocks. The blends contained spherical micelles with S cores and B corona, and two-step relaxation composed of fast and slow processes was observed. This study mainly examined features of the fast process that were not specified in the previous study. When the neighboring micelles were entangled through their corona blocks, a nearly universal relationship was found between reduced moduli for the fast process, $G_r^* = [M_{bB}/c_{bB}RT]G^*$, and reduced frequencies, $\omega\tau^*$, with c_{bB} and M_{bB} being the concentration of the B blocks in the hB matrix and B block molecular weight, respectively, and τ^* being the relaxation time for the fast process. In addition, τ^* was found to increase exponentially with M_{bB}/M_e, with M_e being the entanglement spacing. These features of the fast process were qualitatively the same as those for relaxation of entangled star chains, strongly suggesting that the fast process corresponded to star-like relaxation (arm-retraction) of entangled B blocks being tethered on the S cores. Quantitatively, τ^* for the B blocks were 3−4 orders of magnitude longer than the relaxation times of corresponding star hB chains. This difference was related to effects of the S cores that worked as an impenetrable wall and constrained the B block relaxation. For the slow relaxation process of the SB micellar blends, the relaxation times τ_s were compared with characteristic times for Stokes−Einstein (SE) diffusion of the micelles $\tau_{SE} = \pi R_m \eta_{eff} \delta^2/kT$, with R_m and δ being the micelle radius and diffusion distance, respectively, and η_{eff} being an effective viscosity for micelle diffusion. For concentrated micelles being entangled through their B blocks, τ_s were close to τ_{SE} with δ and η_{eff} being taken as the micelle diameter ($2R_m$) and a viscosity η_{fast} for the fast process of the micelles (relaxation of individual B blocks). This result strongly suggested that the slow process for those entangled micelles corresponded to the SE diffusion of micelles, being in harmony with the previous assignment. However, for dilute, nonentangled micelles, τ_s were significantly shorter than τ_{SE}. This result suggested changes in the molecular mechanism for the slow process with the extent of entanglements between the micelles.

I. Introduction

Rheological properties of block copolymers are strongly influenced by microdomain structures. These structures are in turn determined by the block composition and architecture, temperature (or segregation power), and concentration and solvent quality (for the cases of copolymer solutions).[1] Thus, block copolymers offer a rich field in rheology, and extensive studies have been carried out to elucidate effects of structures on dynamic properties of the copolymer systems.[2−23]

More than ten years ago, Watanabe et al.[9−15] focused their attention to diblock copolymer solutions in *selective* solvents and carried out systematic studies for the structure−rheology relationships. For styrene−butadiene (SB) diblock copolymers being dissolved in a B-selective solvent (*n*-tetradecane) and forming spherical micelles with S cores and B corona, Watanabe et al. found that plasticity emerges when the micelles form a so-called macrolattice having a long-range order.[9] The macrolattice formation was considered to result from balance of contradicting thermodynamic requirements for the corona B blocks, an osmotic requirement of uniform distribution of the B segments in the corona phase and an elastic requirement of randomized B block conformation. This hypothesis was evidenced from several experimental facts,[10−13] including a fact that blends of SB copolymers in a B-selective, *polymeric* solvent, homopolybutadiene (hB), contain *randomly dispersed* micelles (no macrolattice) and exhibit no plasticity.[11,12] Since the hB molecules work as a buffer preserving uniform B segment distribution in the corona phase, the B blocks can take randomized conformation without violating the osmotic requirement and thus the driving force for the macrolattice formation vanishes.

The SB/hB blends have no plasticity and relax viscoelastically (unless the SB content is large). Watanabe et al.[11,14,15] found that the blends relax in two steps and the slow relaxation process is many orders of magnitudes slower than the relaxation process expected for individual B blocks. They attributed this extraordinarily slow process to diffusion of micelles. However, they did not specify features of the fast process.

The micellar diffusion considered by Watanabe et al. is a collective mode of motion for the copolymer chains. We naturally expect that relaxation of individual chains would have taken place at shorter time scales and may have corresponded to the fast process observed for the SB/hB blends. For related systems, binary homopolymer blends[24−37] and entangled star chains,[38−48] extensive viscoelastic data have been accumulated in particular for these ten years, and we can now examine this expectation on the basis of those data.

From this point of view, we have reanalyzed the previous data[14,15] for the SB/hB blends and examined viscoelastic features of the blends in particular for their fast relaxation process. The results are presented in this series of papers. Part 1 (this paper) examines the viscoelastic behavior of the SB micelles in a nonentangling, low molecular weight hB matrix. Specifically,

[⊗] Abstract published in *Advance ACS Abstracts,* December 1, 1995.

0024-9297/96/2229-0104$12.00/0

Table 1. Characteristics of SB and hB Samples

code[a]	$10^{-3}M_S$	$10^{-3}M_B$	M_W/M_n
	SB Diblock Copolymer[b]		
SB 20−46 (SB1)	20	46	1.06
SB 20−97 (SB2)	20	97	1.07
SB 32−102 (SB3)	32	102	1.07
SB 32−160 (SB4)	32	160	1.08
SB 32−262 (SB5)	32	262	1.10
	hB Matrix		
chB−2[c] (chB)		2	2

[a] Parentheses indicate the previously used sample code.[14] [b] 1,2-Vinyl:1,4-cis:1,4-trans ≅ 10:40:50 for B blocks. [c] 1,2-Vinyl:1,4-cis/trans = 83:17.

relaxation times and mode distribution for the fast process of the blends are compared with those for star hB chains.[42−44] Part 2 (following paper) specifies the behavior of the micelles in entangling, high molecular weight hB matrices. Data for entangled homopolymer blends are used to discuss constraint release relaxation[25−37] for the micelles.

II. Experimental Section

II.1. Materials. Table 1 summarizes the molecular characteristics of the styrene−butadiene (SB) diblock copolymers and homopolybutadiene (hB) samples used in a previous study.[14] The SB samples were anionically synthesized in benzene, and their B blocks had the typical microstructure 1,2-vinyl:1,4-cis:1,4-trans ≅ 10:40:50. For the chB-2 sample (a commercially available sample; PB 2000 obtained from Nisseki Co.), the content of the 1,2-linkage was reported to be more than 70%.[49] In this study, the microstructure of chB-2 was quantified from ^{1}H NMR. The result was 1,2-vinyl:1,4-cis/trans = 83:17.

II.2. Correction of Segmental Friction. The previous study examined viscoelastic behavior of blends of the SB copolymers in chB-2.[14] The blends contained spherical micelles with S cores and B corona, and the B blocks were not very concentrated in the corona phase (less than 10 vol % for most cases). Thus, the segmental friction ζ of the 1,4-rich B blocks was essentially determined by the 1,2-rich chB-2 matrix, as evidenced from the coincidence of the time−temperature shift factors a_T for the blends and chB-2.[14]

This study compares the relaxation behavior of the 1,4-B blocks in chB-2 with the behavior of bulk star 1,4-hB chains, the latter being reported in literature.[42−44] Since ζ changes with the content of 1,2-linkage, this comparison requires a correction for ζ in chB-2. For this purpose, we measured storage and loss moduli, G' and G'', for blends of monodisperse linear 1,4-hB chains in chB-2 with RMS 650 (Rheometrics) at 25 °C, a reference temperature previously used for the SB/chB-2 blends.[14] Those hB chains were synthesized in a recent study[50] and had M_{hB} = 39K, 76K, and 152K (1,2-vinyl:1,4-cis:1,4-trans ≅ 10:40:50). The hB volume fraction in the blends, ϕ_{hB}, were 6 and 12 vol % (for M_{hB} = 39K), 4 vol % (for M_{hb} = 76K), and 2 vol % (for M_{hB} = 152K). At these ϕ_{hB}, the hB chains were not entangled among themselves and exhibited Rouse-like behavior. (The matrix chB-2 chains were sufficiently short and not entangled with the hB chains.) ζ for those dilute hB chains was essentially determined by the matrix chB-2, as was the case also for the previously examined SB/chB-2 blends.

The above measurements used the chB-2 sample that has been stabilized with an antioxidant (2,6-di-*tert*-butyl-4-methylphenol), sealed from air, and stored in a freezer for more than ten years (after one of the authors used it in the previous study[14]). For testing the quality of this sample, G^* was measured in this study also for this chB-2 sample. The result was in very good agreement (within a few percent) with the previous data, indicating that the chB-2 sample has been stored without degradation.

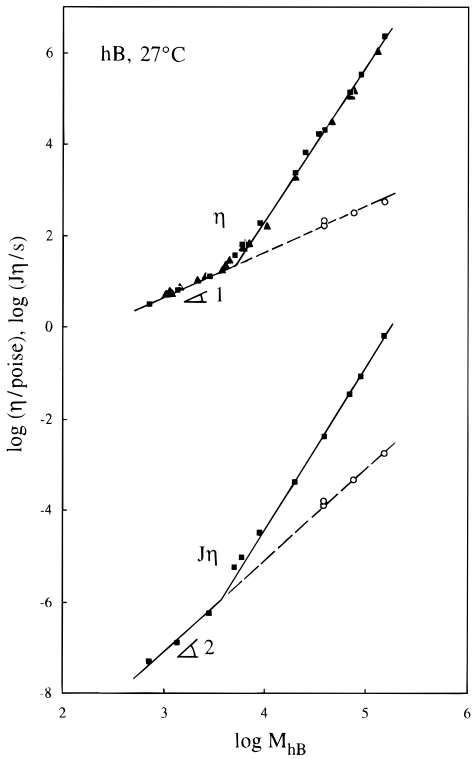

Figure 1. Molecular weight dependence of relaxation time $J\eta$ and viscosity η for bulk, linear 1,4-hB chains at 27 °C. Correction for monomeric friction, ζ, is carried out for low-M chains. Filled squares and triangles indicate the data reported by Watanabe et al.[50b] and Colby et al.[51] The unfilled circles indicate the relaxation time $J_{hB}\eta_{hB}$ and reduced viscosity η_{hB}/ϕ_{hB} for dilute 1,4-hB chains in chB-2 at 25 °C, both being multiplied by a factor of 0.1 as the ζ correction.

From G' and G'' of the hB/chB-2 blends, we subtracted contributions of the chB-2 matrix and evaluated viscosity η_{hB} and compliance J_{hB} of the dilute hB chains. In Figure 1, the relaxation time and reduced viscosity of those hB chains in chB-2 at 25 °C, $J_{hB}\eta_{hB}$ and η_{hB}/ϕ_{hB}, are *multiplied by a factor of 0.1* and plotted against M_{hB} (open circles). The filled symbols indicate the viscosity η and relaxation time $J\eta$ of bulk, linear 1,4-hB chains[50,51] reduced at 27 °C, a reference temperature for star 1,4-hB chains used by Roovers et al.[43,44]

In Figure 1, WLF analysis was carried out for bulk 1,4-hB chains of M_{hB} < 9K to correct their ζ.[50,51] Thus, those low-M chains exhibit the well-known Rouse behavior, $\eta \propto M$ and $J\eta \propto M^2$. The data for the 1,4-hB chains in chB-2 (open circles) are described by the dashed lines that represent extrapolation of this Rouse behavior. This result means that ζ_{in-chB} for the 1,4-hB chains in chB-2 at 25 °C is larger by a factor of 10 than $\zeta_{bulk-1,4}$ for bulk 1,4-hB at 27 °C. In addition, close coincidence of the data for M = 39K at ϕ_{hB} = 6 and 12 vol % indicates that ζ_{in-chB} is insensitive to ϕ_{hB} in a range of $\phi_{hB} \leq$ 12 vol %. For the previously examined SB/chB-2 blends,[14] ϕ_{bB} of the B blocks in the corona phase were mostly in this range. Thus, in the remaining part of this paper, the previous data[14] for the SB/chB-2 blends are corrected with a factor $\zeta_{in-chB}/\zeta_{bulk-1,4}$ = 10 and compared at an iso-ζ state with the data for bulk 1,4-hB stars[42−44] at 27 °C.

III. Results

III.1. Relaxation Mode Distribution. Figure 2 shows representative G' and G'' data obtained in a previous study[14] for SB 20−46/chB-2 blends of various SB content c_{SB}. Spherical micelles with S cores and B corona are formed in the blends.[14] As seen in Figure 2, the blends with large c_{SB} exhibit fast and slow relaxation

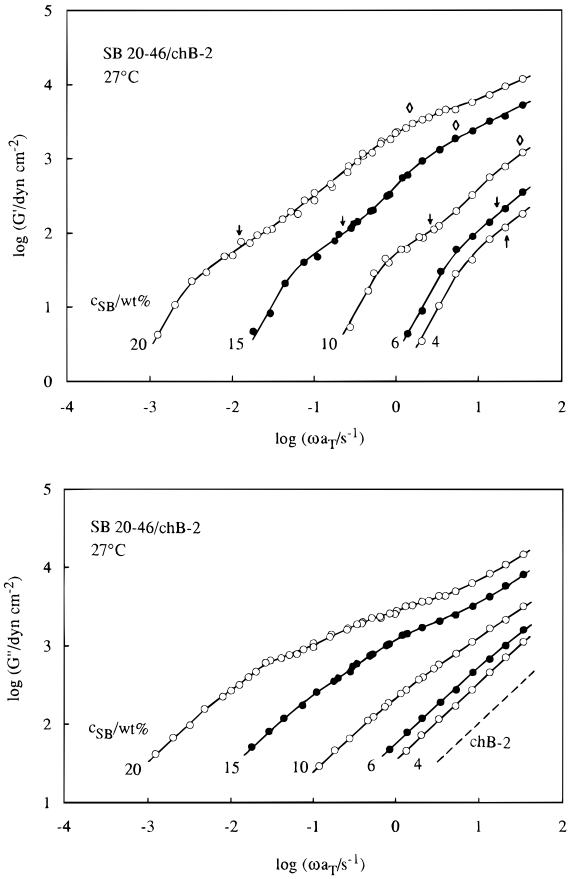

Figure 2. Frequency dependence of G' (top) and G'' (bottom) for SB 20−46/chB-2 blends[14] reduced at an iso-ζ state for bulk 1,4-hB (27 °C). Diamonds and arrows indicate characteristic frequencies, τ^{*-1} and τ_s^{-1}, for the fast and slow processes, respectively.

processes (indicated with the diamonds and arrows, respectively). The previous study[14] attributed the slow process to micelle diffusion but did not specify features of the fast process. At ω examined here, the chB-2 matrix barely contributes to G^* of the blends with large c_{SB} while the rigid S cores lead to no appreciable relaxation. Thus, we may relate the fast process to relaxation of individual B blocks tethered on the S cores. In the remaining part of this paper, we mostly focus our attention to the fast process and test this molecular picture.

In Figure 2, we note that the fast process is shifted to the lower-ω side with increasing $c_{SB} \geq 10$ wt %. For these c_{SB}, the B block concentration c_{bB} in the corona phase is well above the entanglement threshold $c_e = \varrho_{bulk} M_e^0 / M_{bB}$, with ϱ_{bulk} and M_e^0 being the density and entanglement spacing for bulk 1,4-hB and M_{bB} being the B block molecular weight. Thus, the shifts seen for $c_{SB} \geq 10$ wt % are related to entanglement between the B blocks of neighboring micelles. (The short chB-2 matrix chains are not entangled with the B blocks.) Since the B blocks are tethered on the rigid S cores, we expect similarities in the relaxation behavior for the B blocks and multiarm star hB chains.

In the terminal relaxation zone, entangled star chains exhibit a nearly universal relationship between reduced moduli $G_r^* = [M_a/cRT]G^*$ and reduced frequency $\omega\tau$, with M_a, c, RT, and τ being the arm molecular weight, concentration, thermal energy, and relaxation time.[42] This means that the terminal relaxation mode distribution (observed as shape of $G^*(\omega)$ curves in double-logarithmic scales) is nearly universal for the entangled

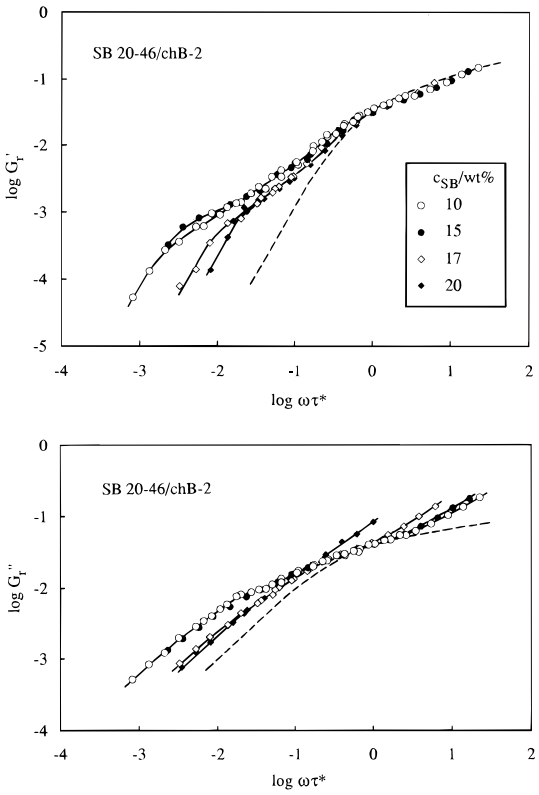

Figure 3. Plots of reduced moduli $G_r^* = [M_{bB}/c_{bB}RT]G^*$ against reduced frequencies $\omega\tau^*$ for the SB 20−46/chB-2 blends containing micelles entangled through the corona B blocks. The dashed curves indicate reduced moduli for entangled 4-arm star 1,4-hB (M_a = 48K)[42] being multiplied by a factor of $^1/_{20}$ and plotted against $\omega\tau$ (τ = star relaxation time).

star chains. Thus, it is informative to examine whether the fast relaxation of the blends exhibits similar universality for $G_r^* = [M_{bB}/c_{bB}RT]G^*$. (At the frequencies examined here, G^* of the blends with large c_{SB} have negligible contribution from the short chB-2 matrix and are very close to G^*_{SB} of the SB copolymers.)

Figure 3 compares the G_r^* curves for the entangled SB 20−46/chB-2 blends ($c_{bB} > c_e$). The curves are shifted along the ω axis by factors τ^* so that they are best superposed with each other in the fast relaxation regime at around $\omega\tau^* = 1$. We note good superposition for G_r' at $\omega\tau^* \geq 1$. Since contribution of very rapid relaxation at $\omega\tau^* \geq 100$ is much larger for G_r'' than for G_r', poorer superposition is observed for G_r''. However, subtraction of this contribution improved the superposition for G_r''. These results demonstrate nearly identical shape of the G_r^* curves (nearly universal mode distribution) for the fast process of the SB 20−46 micelles of various c_{SB} (≥ 10 wt %).

In Figure 3, the G_r^* data for the SB 20−46 blends are also compared with those for bulk, 4-arm star 1,4-hB examined by Raju et al.[42] This entangled star hB has M_a (= 48K) being close to M_{bB} (= 46K) for the SB 20−46 copolymer, and its G_r^* were found to be ≅20 times larger in magnitude than G_r^* of the SB 20−46 blends. At this moment, no clear explanation is found for this difference in the magnitude of G_r^*. Keeping this puzzling difference in mind, we indicated $G_r^*/20$ *vs* $\omega\tau$ plots for the star hB with the dashed curves in Figure 3, where τ (= $J\eta$) is the terminal relaxation time of the star hB (at 27 °C).[42] Comparison with these curves is sufficient for examining relative distribution of viscoelastic modes for the SB micelles. Clearly, the G_r^* curves of the blends are close to the dashed curves. This

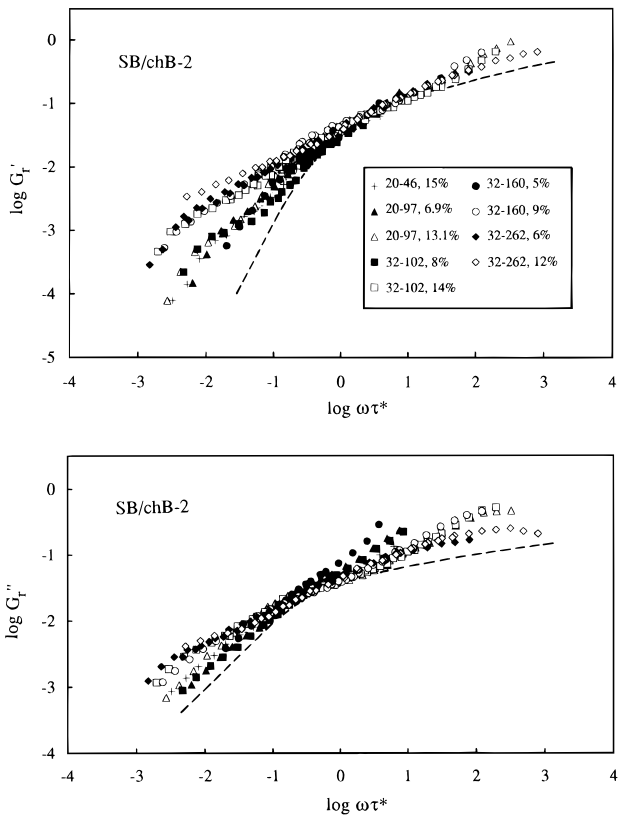

Figure 4. Comparison of reduced moduli $G_r^* = [M_{bB}/c_{bB}RT]$-$G^*$ plotted against reduced frequencies $\omega\tau^*$ for various SB/chB-2 blends as indicated. The blends contained micelles being entangled through the B blocks. For SB 32−160 and 32−262 copolymers having small S content, G_r^* are multiplied by factors of 0.8 and 0.2, respectively. The dashed curves are the same as in Figure 3.

result means that the relative mode distribution is nearly the same for the terminal relaxation of the star hB and the fast process of the blends.

Figure 4 compares representative G_r^* data[14] for entangled micellar blends ($c_{bB} > c_e$) of various M_{bB} (cf. Table 1). As in Figure 3, the G_r^* curves were shifted along the ω axis by factors τ^* to achieve the best superposition at around $\omega\tau^* = 1$. Magnitudes of G_r^* were nearly the same for the SB 20−46, 20−97, and 32−102 copolymers having relatively large S content (ϕ_S) but were larger for SB 32−160 and 32−262 with smaller ϕ_S. Again, no clear explanation is found for this difference. In Figure 4, G_r^* for the last two cpolymers were multiplied by factors of 0.8 and 0.2, respectively, and only the relative distribution of the viscoelastic modes is compared for the five copolymers. The dashed curves are the same as those in Figure 3.

As seen in Figure 4, reasonably good superposition is achieved for the G_r' curves at $\omega\tau^* \geq 1$ for the entangled micelles of various M_{bB} and the star hB (dashed curves). (The superposition for G_r'' was improved by subtraction of the contribution from very rapid relaxation, as was the case also for Figure 3.) Thus, the relative distribution of the viscoelastic modes for the fast process appears to be insensitive to M_{bB} and c_{bB} and close to that for the star-hB. This result and those seen in Figure 3 indicate that the fast process due to entanglement relaxation of individual B blocks is similar in nature to relaxation of entangled star chains.

In Figures 3 and 4, we also note that the G_r^* curves are not universally superposed at $\omega\tau^* < 1$ where the slow process is observed. This result suggests that the

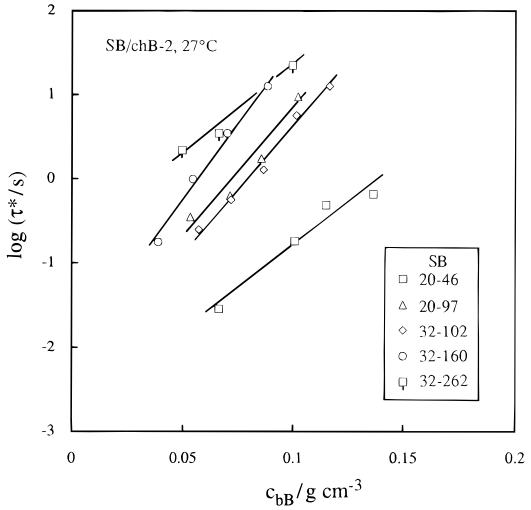

Figure 5. Dependence of the relaxation time τ^* for the fast process of SB/chB-2 micellar blends on the B block concentration c_{bB} in the matrix phase. The τ^* data are reduced at an iso-ζ state for bulk 1,4-hB (27 °C).

fast and slow processes have different relaxation mechanisms, as discussed later in more detail.

III.2. Relaxation Time for Fast Process. In Figures 3 and 4, ω for the star hB is scaled with the relaxation time, $\tau = J_{star}\eta_{star}$. Thus, the superposition of the G_r^* curves for the blends and star hB on the $\omega\tau$ and $\omega\tau^*$ scales means that τ^* can be used as the relaxation time for the fast process of the blends. In fact, characteristic frequencies $1/\tau^*$ (diamonds in Figure 2) are located at around the low-ω end of the fast process. In general, it is not very easy to accurately determine a characteristic time for a relaxation process being followed by slower processes, and τ^* determined in Figures 3 and 4 may contain uncertainties as large as $\Delta \log \tau^* = 0.3$. However, those τ^* data are still sufficient for the following argument.

For blends containing micelles being entangled through the B blocks ($c_{bB} > c_e$), Figure 5 shows semilogarithmic plots of τ^* against the B block concentration, c_{bB}. We note that τ^* increases exponentially with c_{bB}, but the increasing rate is different for micelles of different M_{bB}.

The exponential c dependence of the relaxation time is characteristic to relaxation of entangled star chains: Extensive τ data accumulated for well-entangled star chains[38−44,46,48] are summarized as

$$\tau = J\eta \propto \exp(\nu' M_a/M_e) \qquad (1)$$

with ν' being a constant somewhat smaller than unity. (A weakly M_a-dependent prefactor is neglected in eq 1.) For entangled solutions of star chains, M_e scales as $c^{-\beta}$ with β being a constant close to (or a little larger than) unity. This leads to the exponential c dependence of τ, as should be the case also for τ^* of the micellar blends (Figure 5).

Equation 1 indicates that τ for entangled star chains of various c and M_a are (almost) universally dependent on the M_a/M_e ratio. For testing this universality for entangled micellar blends, Figure 6 examines M_{bB}/M_e dependence of their τ^*. Here, M_e for the B blocks in the chB-2 matrix was estimated as $M_e = M_e^0 Q_{bulk}/c_{bB}$. For blends of the SB 20−46, 20−97, and 32−102 copolymers having relatively large S content ϕ_S, τ^* appears to universally depend on M_{bB}/M_e and this dependence can be approximated as an exponential dependence for large M_{bB}/M_e. Thus, those blends ex-

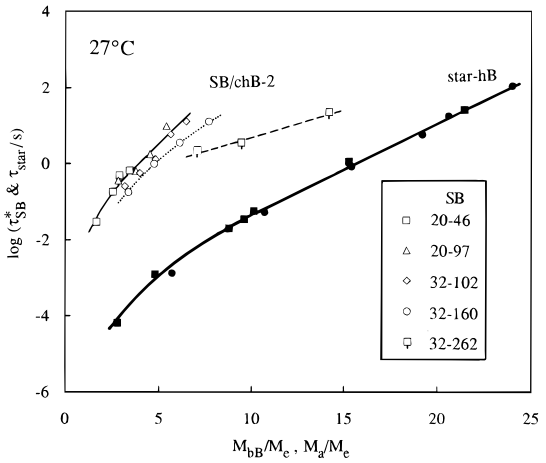

Figure 6. Dependence of the relaxation time τ^* for the fast process of SB/chB-2 micellar blends on M_{bB}/M_e ratio (unfilled symbols). The filled circles and squares indicate τ data reduced at 27 °C for entangled 4-arm[42,43] and 18-arm[44] star 1,4-hB. The τ^* data for the blends are compared with those τ data at the iso-ζ state.

hibit features characteristic to entangled star chains. However, τ^* becomes smaller for the SB 32−160 and 32−262 copolymers having smaller ϕ_S. This break of the universal M_{bB}/M_e dependence of τ^* may be related to effects of S cores, as discussed later in section IV.1.

In Figure 6, the filled symbols indicate τ_{star} data (reduced at 27 °C) reported by Raju et al.[42] (for 4-arm star hB) and by Roovers et al.[43,44] (for 4- and 18-arm star hB). Clearly, τ^* for the B blocks are 3−4 orders of magnitude larger than τ_{star}. This fact indicates that the relaxation mechanism is similar but not completely the same for the B blocks and star hB.

IV. Discussion

IV.1. Fast Relaxation of SB/chB Blends. In the previous section, we found similarities for the entangled micelles with large ϕ_S and star hB, nearly universal G_r^* curves being scaled with a factor of $M_{bB}/c_{bB}RT$ (Figures 3 and 4) and nearly exponential dependence of τ^* on M_{bB}/M_e (Figure 6). From these similarities, we can attribute the fast relaxation process of those micelles to starlike relaxation of entangled B blocks tethered on the S cores. However, for the micelles and star hB, we also found quantitative differences of τ^*_{SB} and τ_{star} (Figure 6). In addition, the above universalities vanish for small ϕ_S. These results suggest that the S cores (not existing for star hB) have important effects on the B block relaxation and the effects change with the core size. A previous analysis[14,15] did not consider those effects and was incomplete. We here consider the effects of the S cores within a context of the tube model,[52−54] and reexamine the relaxation mechanism for the B blocks.

Tube Model for B Blocks. For entangled star chains, the tube model considers that the star arm trapped in a tube relaxes when it retracts along the tube.[52−54] The retraction leads to a decrease in conformational entropy that provides an activation barrier for the arm relaxation. The barrier $U(L)$ increases with decreasing contour length L of the arm measured along the tube, and the relaxation time τ is essentially scaled as $\exp[\Delta U(\xi)/kT]$.[52−54] Here, $\Delta U(L) = U(L) - U(L_{eq})$, L_{eq} is an equilibrium L value, and ξ indicates a small, characteristic contour length to which the arm has to retract for complete escape from the tube. This *escape length*, ξ, should be close to the size of an entanglement segment, $a = \nu b n_e^{1/2}$, where ν, n_e, and b denote a numerical constant close to unity, the number of monomeric segments between entanglements, and the step length of those segments, respectively.

For a star arm composed of n_a monomeric segments, the Doi−Kuzuu (DK)[53] and Pearson−Helfand (PH)[54] models assume a quadratic U^0 having the minimum at $L = L_{eq}{}^0$,

$$U^0(L) = \alpha kT[1 - (L/L_{eq}{}^0)]^2 + U^0(L_{eq}{}^0), \quad \alpha = (3\nu^2/2)(n_a/n_e) \quad (2)$$

Here, the equilibrium $L_{eq}{}^0$ is given by

$$L_{eq}{}^0 = \nu b n_a/n_e{}^{1/2} \quad (3)$$

For U^0 given in eq 2, the DK and PH models predict that τ and η of well-entangled star chains increase exponentially with M_a/M_e (cf. eq 1) while J increases in proportion to M_a/M_e.[52−54] (In these models, ξ is much smaller than $L_{eq}{}^0$ and $\Delta U(\xi)/kT$ is proportional to $n_a/n_e = M_a/M_e$.) These predictions are in good agreement with experiments.[43,44,46,48,54] In addition, the PH model excellently describes the viscoelastic mode distribution (shape of G^* curves).[54] For 1,4-hB star chains, Roovers et al.[43,44] reported agreements between experiments and the PH prediction with a parameter $\nu' = 3\nu^2/2 = 0.5$. A difference between this ν' value and the value originally expected for $L_{eq}{}^0$, $\nu' \cong 1.5$ (for $\nu \cong 1$), may be related to significant constraint release effects existing even for well-entangled star chains.[32,55] Except this point, the tube models have been successfully used for describing the relaxation of entangled star chains.

Now, we note an important difference between the B blocks of the SB micelles and the star arm. The entropic barrier for the latter (eq 2) is obtained from a Gaussian distribution function $\Psi^0(L)$ as

$$U^0(L) = -kT \ln \Psi^0(L) - F_{eq}L, \quad \Psi^0(L) \propto \exp[-3L^2/2n_a b^2] \quad (4)$$

Here, F_{eq} is a fictitious force[53] that is adjusted to locate the minimum of $U^0(L)$ at $L = L_{eq}{}^0$. The function $\Psi^0(L)$ is in turn obtained for an end-grafted chain *having no impenetrable domain*. Since the micelle S cores are impenetrable for the B blocks, the distribution function $\Psi(L)$ for the B blocks should be different from $\Psi^0(L)$.

We here consider micelles having S cores and B corona layers of comparable size. For these micelles, the effects of the S cores on Ψ would not be significant unless the B block trapped in a tube retracts to a vicinity of the core. Thus, for large L, the entropic barrier $U(L)$ for the B block would not be very different from $U^0(L)$ for the star arm. However, for small L, the S cores can be regarded as a flat, impenetrable wall for the B block and $\Psi(L)$ would be approximated by a standard distribution function for a chain tethered on an infinitely large, flat wall,[56]

$$\Psi(L) \propto L \exp[-3L^2/2n_a b^2] \text{ for small } L \quad (5)$$

Considering the wall effects,[56] we may approximate L_{eq} as $2^{1/2}L_{eq}{}^0 = 2^{1/2}\nu b n_a/n_e{}^{1/2}$. Then, from eq 5, we can

Table 2. Comparison of d_S of the S Cores and $R_{B,\theta}$ of the B Block for SB Micelles

SB	d_S (Å)	$R_{B,\theta}$ (Å)
SB 20−46	206	196
SB 20−97	208	284
SB 32−102	250	291
SB 32−160	260	365
SB 32−262	270	467

estimate $U(L)$ *for small* L as

$$U(L) = -kT \ln \Psi(L) - F_{eq}L$$
$$= 2\alpha kT[1 - (L/L_{eq})]^2 + kT[(L/L_{eq}) - 1 - \ln(L/L_{eq})] + U(L_{eq}), \quad \alpha = (3\nu^2/2)(n_a/n_e) \quad (6)$$

Here, F_{eq} is adjusted to locate the minimum of $U(L)$ at $L = L_{eq}$, as done in the DK model.[53] Equation 6 indicates that the wall effect leads to logarithmic divergence of $U(L)$ for $L \to 0$.

As can be noted from eqs 2 and 6, $U(L)$ is significantly larger than $U^0(L)$ for small L. Since τ is essentially scaled as $\exp[\Delta U(\xi)/kT]$ with ξ being the small escape length, this difference between U and U^0 suggests that τ is significantly longer for the chain tethered on the flat, impenetrable wall than for the end-grafted chain having no impenetrable domain.

Comparison with Tube Model. Table 2 summarizes the diameter of the S cores and the unperturbed end-to-end distance of the B blocks, d_S and $R_{B,\theta}$, for the micelles of the five SB copolymers (cf. Table 1). For 10 wt % micellar solutions of these SB copolymers in a B-selective solvent, *n*-tetradecane (C14), d_S was determined at 25 °C (at strongly segregated state) from SAXS measurements.[10] Those d_S values were consistent with d_S data for bulk SB copolymers of smaller M.[57] Thus, in Table 2, we used the d_S for the 10 wt % SB/C14 systems as d_S for the SB/chB-2 blends.

For the SB 20−46, 20−97, and 32−102 micelles having relatively large S content (ϕ_S), d_S is comparable with $R_{B,\theta}$ (Table 2) and the argument for the tethered chains on the *flat*, impenetrable wall (eqs 5 and 6) appears to be valid. Thus, the differences between τ^* of these micelles and the star hB (Figure 6) would be due to the S cores that behave as the flat wall and constrain the B block relaxation at small L. On the other hand, d_S is considerably smaller than $R_{B,\theta}$ for the SB 32−160 and 32−262 micelles with smaller ϕ_S. For these micelles, the *S* cores would not behave as the flat wall and eqs 5 and 6 would not be valid. In other words, the constraint from the S cores for the B block relaxation is weaker for these micelles than for the above micelles having $d_S \cong R_{B,\theta}$. This would have led to the break of the universality of τ^* at small ϕ_S (Figure 6). (The difference in the constraint from the S cores might also have led to the differences in magnitudes of G_r^* (Figures 3 and 4), but it is not clearly understood yet how the strength of the contraint affects the G_r^* magnitude.)

Rigorous calculation of the viscoelastic quantities for the B block requires us to solve a time evolution equation for a probability density of tube survival.[54] However, $U(L)$ to be incorporated in this equation is not known for the SB copolymers with small ϕ_S, and even for large ϕ_S an approximate $U(L)$ (eq 6) is found only for small L. Thus, in this paper, we analyze the relaxation time τ^* only in an approximate way.

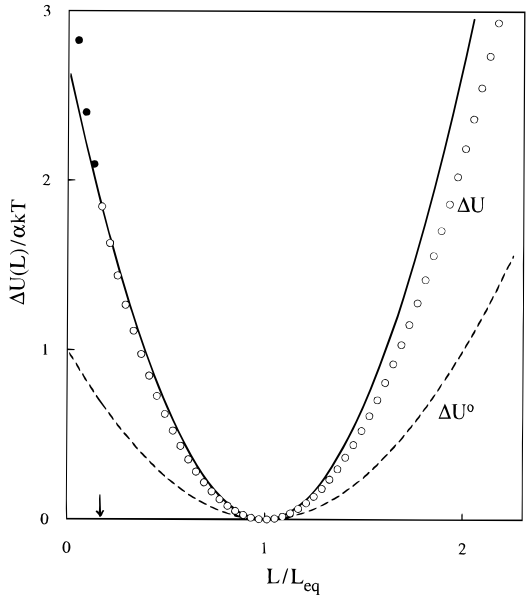

Figure 7. Entropic barrier for escape of a chain (with $\alpha = \nu' n_a/n_e = 2$) being trapped in a tube. The circles indicate $\Delta U(L)$ for the chain tethered on a flat, impenetrable wall, and the dashed curve denotes $\Delta U^0(L)$ for the end-grafted chain having no impenetrable domain. The solid curve represents a quadratic function, $(\nu'_{eff}/\nu')\Delta U^0(L)$. The arrow indicates a reduced escape length, $\xi/L_{eq} = a/L_{eq}$.

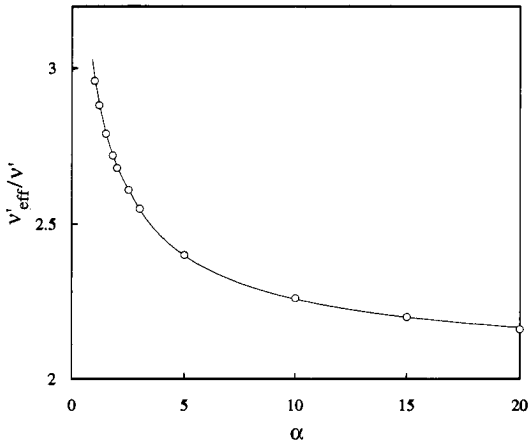

Figure 8. Dependence of the ν'_{eff}/ν' coefficient for an approximate $\Delta U(L)$ on $\alpha = \nu' n_a/n_e$.

In this analysis, we compared $\Delta U(L)$ and $\Delta U^0(L)$ for the B block and the star arm having the same n_a. Figure 7 shows an example for $\alpha = \nu' n_a/n_e = 2$ ($\nu' = 3\nu^2/2$; cf. eqs 2 and 6). As seen there, $\Delta U(L)$ (circle) is larger than $\Delta U^0(L)$ (dashed curve) in the entire range of L. However, in a range $\xi < L < L_{eq}$ with the escape length being taken as $\xi = a = \nu b n_e^{1/2}$ (indicated with the arrow), $\Delta U(L)$ can be approximated by a quadratic function of L/L_{eq} (solid curve). This function is written in terms of $\Delta U^0(L)$ as $(\nu'_{eff}/\nu')\Delta U^0(L) = \nu'_{eff} kT(n_a/n_e)[1 - (L/L_{eq}^0)]^2$, with ν'_{eff} being an effective ν' value for the approximate $\Delta U(L)$ at $\xi < L < L_{eq}$. For other α values, $\Delta U(L)$ was also approximated by the quadratic function, $(\nu'_{eff}/\nu')\Delta U^0(L)$, and the ν'_{eff}/ν' ratio monotonically decreased with increasing α (Figure 8).

From the results of Figures 7 and 8, we expect that τ^*_{SB} for the entangled B blocks is approximately proportional to $\exp[(\nu'_{eff}/\nu')\Delta U^0(\xi)/kT]$ and thus the dependence of τ^*_{SB} on $\nu'_{eff} M_{bB}/M_e$ is close to the dependence of τ_{star} on $\nu' M_a/M_e$ (cf. eq 2). This expectation is examined in Figure 9 where τ^*_{SB} and τ_{star} are plotted

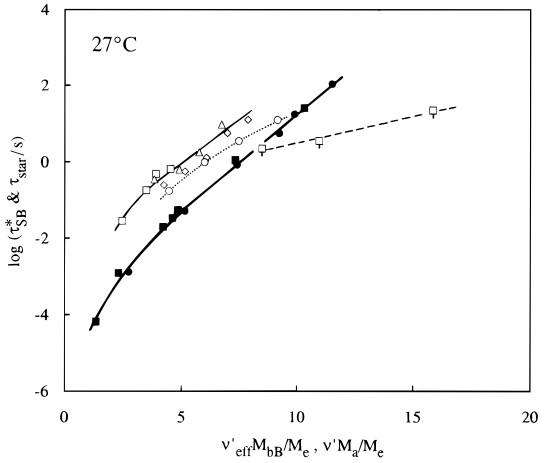

Figure 9. Plots of the relaxation time τ^*_{SB} for the fast process of SB/chB-2 micellar blends against $\nu'_{eff}M_{bB}/M_e$. The symbols are the same as in Figure 6.

against $\nu'_{eff}M_{bB}/M_e$ and $\nu'M_a/M_e$, respectively. The symbols are the same as in Figure 6. The ν'_{eff} values for τ^*_{SB} were evaluated from Figure 8.

As explained for Table 2, the S cores can be regarded as the flat, impenetrable wall for the B blocks only when d_S is comparable with (or larger than) $R_{B,\theta}$. Thus, the above approximation (being valid for large S cores), $\Delta U(L) \cong (\nu'_{eff}/\nu')\Delta U^0(L)$, should lead to over-reduction of τ^*_{SB} when d_S is considerably smaller than $R_{B,\theta}$. This over-reduction is seen in Figure 9 for SB 32−262 with $d_S \cong 0.6R_{B,\theta}$ (squares with pips). On the other hand, for the entangled micelles with $d_S \cong R_{B,\theta}$, the differences seen in Figure 6 for τ_{star} and τ^*_{SB} are largely reduced in Figure 9. This result qualitatively supports the above expectation, suggesting that the differences between the SB micelles and star hB are essentially due to the constraint from the S cores.

However, in Figure 9, we also note nontrivial differences between τ_{star} and τ^*_{SB} even for the micelles with $d_S \cong R_{B,\theta}$. These differences might be partly related to uncertainties in the escape length, ξ: For example, the differences almost disappeared when we assumed a smaller ξ of $0.5\nu b n_e^{1/2}$ and evaluated ν'_{eff} accordingly (cf. Figures 7 and 8). More importantly, the analysis for the B blocks (eqs 5 and 6) does not consider effects of S cores of *neighboring* micelles. Incorporation of these effects in the analysis may also reduce the differences of τ_{star} and τ^*_{SB} noted in Figure 9. Thus, it is desired to derive a complete expression of $U(L)$, formulate a tube model for the B block that is constrained by this U(L), and compare the resulting viscoelastic quantities of the B blocks with those of entangled star chains. This rigorous calculation is considered as interesting future work.

IV.2. Slow Relaxation of SB/chB Blends. In the G_r^* vs $\omega\tau^*$ plots shown in Figures 3 and 4, the fast relaxation process of the SB micellar blends exhibits nearly universal mode distribution while the slow process does not. This result suggests differences in the relaxation mechanism for the two processes. In the previous work, the slow process for the entangled blends was attributed to diffusion of the micelles:[14] Spatial distribution of the micelles becomes anisotropic, generating stress when the blends are deformed, and the micelle diffusion is required to recover the isotropic distribution and induce stress relaxation. We here reexamine this molecular picture.

If the slow process of the blends is governed by the simplest Stokes−Einstein (SE) diffusion mechanism, the relaxation time of this process τ_s should be close to the SE diffusion time,

$$\tau_{SE} = \delta^2/6D_m, \quad D_m = kT/(6\pi R_m \eta_{eff}) \tag{7}$$

Here, δ is a diffusion distance required for the recovery of isotropic distribution of the micelles, R_m is the micelle radius, and η_{eff} is an effective viscosity for the micelle diffusion. R_m was evaluated to be $0.5d_S + 2^{1/2}R_{B,\theta}$ (cf. Table 2), with the factor $2^{1/2}$ accounting for the effects of impenetrable S cores on the B block conformation. For simplicity, δ was taken to be the micelle diameter, $2R_m$.

Estimation of η_{eff} is carried out in the following way. For concentrated micelles being entangled through their B blocks, the micelle diffusion would take place only after individual B blocks relax. In other words, the micelle diffusion rate would be determined by the relaxation of the B blocks observed as the fast process of the blends, suggesting that η_{eff} is given by a viscosity η_{fast} associated to this process. For the entangled SB micelles, Figures 3 and 4 indicate that the G_r^* curves in the fast relaxation regime are close to the adequately scaled G_r^* curves (dashed curves) of the entangled star hB of M_a = 48K. Thus, for those micelles, we determined the η_{fast} values from the known viscosity of the star hB and evaluated τ_{SE} from eq 7 with $\eta_{eff} = \eta_{fast}$.

On the other hand, diffusion of dilute and nonoverlapping SB micelles would not necessarily require complete relaxation of individual corona B blocks, as noted from an example that diffusion takes place even for the dilute micelles having rubbery and nonrelaxing corona layers. Thus, in general, η_{eff} for the dilute SB micelles would have a value between η_{fast} for the B block relaxation and η_{mat} of the pure matrix. However, as an extreme case, we here assume $\eta_{eff} = \eta_{fast}$ and evaluate τ_{SE} from eq 7 also for the dilute, nonentangled micelles (e.g, those with c_{SB} = 4 and 6 wt % in Figure 2). For those micelles, the B block relaxation was not observed in our experimental window (cf. Figure 2). Thus, we assumed the B blocks to behave as tethered Rouse chains and estimated their viscosity, η_{fast}, from the η data for low-M linear hB chains (Figure 1).

In Figure 10, the SE diffusion time τ_{SE} (for $\eta_{eff} = \eta_{fast}$) is compared with characteristic time τ_s for the slow process of the blends. The unfilled and filled symbols indicate the data for micelles having entangled ($M_{bB}/M_e > 2$) and nonentangled ($M_{bB}/M_e \le 2$) B blocks. As done for homopolymer blends,[27−32] τ_s were evaluated from the G* data for the blends and pure chB-2 matrix as

$$\tau_s = J_{SB}\eta_{SB} \tag{8}$$

with

$$\eta_{SB} = \left[\frac{G''_{blend} - \phi_{chB}G''_{chB}}{\omega}\right]_{\omega\to 0} \text{ and } J_{SB} = \frac{1}{\eta_{SB}^2}\left[\frac{G'_{blend} - \phi_{chB}G'_{chB}}{\omega^2}\right]_{\omega\to 0} \tag{9}$$

Here, ϕ_{chB} denotes the volume fraction of chB-2 in the blends and η_{SB} and J_{SB} represent viscosity and compliance of the SB copolymers in the blends, respectively. τ_s gives an average relaxation time (often referred to as a *weight-average* relaxation time) that is close to the longest relaxation time of the blends. In fact, characteristic frequencies τ_s^{-1} (cf. arrows in Figure 2) specify

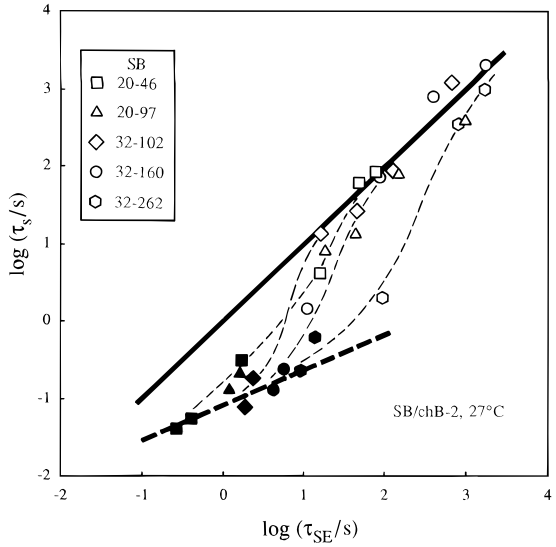

Figure 10. Plots of the relaxation time τ_s for the slow process of SB/chB-2 micellar blends against the Stokes−Einstein diffusion time τ_{SE} evaluated from eq 7 with $\eta_{eff} = \eta_{fast}$. The data are compared at the iso-ζ state for bulk 1,4-hB (27 °C). The filled and unfilled symbols indicate data for micelles having nonentangled ($M_{bB}/M_e \leq 2$) and entangled ($M_{bB}/M_e > 2$) B blocks, respectively. The solid curve indicates a relationship, $\tau_s = \tau_{SE}$.

well the low-ω end of the fast process. (The τ_s values obtained from eqs 8 and 9 were close to the values previously evaluated for numerically calculated relaxation spectra of the blends.[14])

In Figure 10, we note that a relationship between τ_s and τ_{SE} changes with the extent of entanglement: For the nonentangled micelles (filled symbols), τ_s is considerably smaller than τ_{SE} and exhibits weak dependence on τ_{SE} (thick dashed line). This dependence becomes stronger with increasing M_{bB}/M_e (with increasing τ_{SE}). Finally, for well-entangled micelles of various c_{SB} and M_{bB} ($> 4M_e$), τ_s appears to be universally dependent on τ_{SE} and collapsed around the thick solid line representing a relationship, $\tau_s = \tau_{SE}$.

The results of Figure 10 strongly suggest that the slow relaxation process of well-entangled micelles is attributed to their SE diffusion (retarded by entanglements between B blocks), being in harmony with the previous argument.[14] However, the results also indicate that the slow relaxation mechanism may be different for the entangled and nonentangled micelles.

Concerning this difference, one might expect that the relationship $\tau_s = \tau_{SE}$ holds irrespective of the entanglement between the micelles if the diffusion distance δ is taken to be an intermicellar distance δ_m, not the micelle diameter $2R_m$. However, for the blends examined in this paper, the difference in τ_s for the entangled and nonentangled micelles was *magnified* when δ_m was used as δ. Thus, the simple argument of diffusion over the intermicellar distance fails to explain the features of the slow process of the dilute micelles.

One might also expect that the diffusion rate for the dilute micelles is determined by the matrix viscosity η_{mat} and the SE diffusion time $\tau_{SE}°$ evaluated for $\eta_{eff} = \eta_{mat}$ (cf. eq 7) agrees with τ_s for those micelles. This expectation is examined in part 2 of this series of papers for the dilute SB micelles in nonentangling and entangling hB matrices. As shown there, $\tau_{SE}°$ is fairly close to τ_s in the nonentangling chB-2 matrix examined here. However, in the entangling high-M hB matrices, $\tau_{SE}°$ is orders of magnitudes longer than τ_s. Thus, the slow relaxation process of the dilute micelles *might* be attributed to the SE diffusion for the limited case of the nonentangling matrix but not for general cases. Further studies are necessary for this problem.

V. Concluding Remarks

We have examined features of the fast relaxation process for SB/chB-2 blends containing micelles with S cores and B corona. When the S cores are comparable in size with the B corona layers and neighboring micelles are entangled through their B blocks, the fast process exhibited characteristic features, a nearly universal mode distribution of G_r* scaled by a factor of $M_{bB}/c_{bB}RT$ (Figures 3 and 4) and a nearly universal M_{bB}/M_e dependence of τ* that can be approximated as an exponential dependence (Figure 6). These features are similar to those for entangled star chains, strongly suggesting that the fast process corresponds to the starlike relaxation (arm retraction) of the entangled B blocks tethered on the S cores. Analyses in terms of the tube model suggest that quantitative differences found between τ_{SB}* and τ_{star} are related to the effects of the S cores that behave as an impenetrable wall and constrain the B block relaxation (Figure 9).

For the slow process of the entangled micellar blends, the relaxation time τ_s is found to be close to the Stokes−Einstein (SE) diffusion time τ_{SE} evaluated for $\eta_{eff} = \eta_{fast}$ (Figure 10). This result suggests that the slow processes of those micelles correspond to their SE diffusion, being in harmony with the previous assignment. However, for dilute, nonentangled micelles, τ_s are significantly shorter than τ_{SE}. This result may mean that the slow relaxation mechanism changes with the extent of entanglement between the micelles. This problem deserves further attention, and it is desired to compare τ_s with independently measured diffusion times. This comparison is considered as interesting future work.

References and Notes

(1) See, for example: Bates, F. S.; Frederickson, G. H. *Annu. Rev. Phys. Chem.* **1990**, *41*, 525.
(2) Chung, C. I.; Lin, M. I. *J. Polym. Sci., Polym. Phys. Ed.* **1978**, *16*, 545.
(3) Chung, C. I.; Griesbach, H. L.; Young, L. *J. Polym. Sci., Polym. Phys. Ed.* **1980**, *18*, 1237.
(4) Pico, E. R.; Williams, M. C. *Polym. Eng. Sci.* **1977**, *17*, 573.
(5) Gouinlock, E. V.; Porter, R. S. *Polym. Eng. Sci.* **1977**, *17*, 535.
(6) Kotaka, T.; White, J. L. *Trans. Soc. Rheol.* **1973**, *17*, 587.
(7) Osaki, K.; Kim, B. S.; Kurata, M. *Bull. Inst. Chem. Res. Kyoto Univ.* **1978**, *56*, 56.
(8) Masuda, T.; Matsumoto, Y.; Onogi, S. *J. Macromol. Sci., Phys.* **1980**, *B17*, 256.
(9) Watanabe, H.; Kotaka, T.; Hashimoto, T.; Shibayama, M.; Kawai, H. *J. Rheol.* **1982**, *26*, 153.
(10) Watanabe, H.; Kotaka, T. *Polym. J.* **1982**, *14*, 739.
(11) Watanabe, H.; Yamao, S.; Kotaka, T. *J. Soc. Rheol. Jpn.* **1982**, *10*, 143.
(12) Watanabe, H.; Kotaka, T. *J. Rheol.* **1983**, *27*, 223.
(13) Watanabe, H.; Kotaka, T. *Polym. J.* **1983**, *15*, 337.
(14) Watanabe, H.; Kotaka, T. *Macromolecules* **1983**, *16*, 769.
(15) Watanabe, H.; Kotaka, T. *Macromolecules* **1984**, *17*, 342.
(16) Rosedale, J. H.; Bates, F. S. *Macromolecules* **1990**, *23*, 2329.
(17) Koppi, K.; Tirrell, M.; Bates, F. S.; Almdal, K.; Colby, R. H. *J. Phys. II* **1992**, *2*, 1941.
(18) Koppi, K.; Tirrell, M.; Bates, F. S. *Phys. Rev. Lett.* **1993**, *70*, 1449.
(19) (a) Larson, R. G.; Winey, K. I.; Patel, S. S.; Watanabe, H.; Bruinsma, R. *Rheol. Acta* **1993**, *32*, 245. (b) Patel, S. S.; Larson, R. G.; Winey, K. I.; Watanabe, H. *Macromolecules* **1995**, *28*, 4313.
(20) Winey, K. I.; Patel, S. S.; Larson, R. G.; Watanabe, H. *Macromolecules* **1993**, *26*, 2542, 4373.
(21) Morrison, F. A.; Winter, H. H. *Macromolecules* **1989**, *22*, 3533.

(22) Morrison, F. A.; Winter, H. H.; Gronski, W.; Barnes, J. D. *Macromolecules* **1990**, *23*, 4200.
(23) Kannan, R. M.; Kornfield, J. A. *Macromolecules* **1994**, *27*, 1177.
(24) For earlier work on binary polymer blends, see: Ferry, J. D. *Viscoelastic Properties of Polymers*, 3rd ed.; Wiley: New York, 1980; Chapter 13.
(25) Watanabe, H.; Kotaka, T. *Macromolecules* **1984**, *17*, 2316.
(26) Watanabe, H.; Sakamoto, T.; Kotaka, T. *Macromolecules* **1985**, *18*, 1008, 1436.
(27) Watanabe, H.; Kotaka, T. *Macromolecules* **1986**, *19*, 2520.
(28) Watanabe, H.; Yoshida, H.; Kotaka, T. *Macromolecules* **1988**, *21*, 2175.
(29) Yoshida, H.; Watanabe, H.; Kotaka, T. Macromolecules **1991**, *24*, 572.
(30) Watanabe, H.; Yamazaki, M.; Yoshida, H.; Kotaka, T. *Macromolecules* **1991**, *24*, 5573.
(31) Watanabe, H.; Kotaka, T. *CHEMTRACTS Macromol. Chem.* **1991**, *2*, 139.
(32) Watanabe, H.; Yoshida, H.; Kotaka, T. *Macromolecules* **1992**, *25*, 2442.
(33) Montfort, J.-P.; Marin, G.; Monge, P. *Macromolecules* **1984**, *17*, 1551.
(34) Montfort, J.-P.; Marin, G.; Monge, P. *Macromolecules* **1986**, *19*, 1979.
(35) Struglinski, M. J.; Graessley, W. W. *Macromolecules* **1985**, *18*, 2630.
(36) Struglinski, M. J.; Graessley, W. W.; Fetters, L. J. *Macromolecules* **1988**, *21*, 783.
(37) Roovers, J. *Macromolecules* **1987**, *20*, 148.
(38) Masuda, T.; Ohta, Y.; Onogi, S. *Macromolecules* **1971**, *4*, 763.
(39) Graessley, W. W.; Masuda, T.; Roovers, J.; Hadjichristidis, N. *Macromolecules* **1976**, *9*, 127.
(40) Kajiura, H.; Ushiyama, Y.; Fujita, T.; Nagasawa, M. *Macromolecules* **1978**, *11*, 894.
(41) Graessley, W. W.; Roovers, J. *Macromolecules* **1979**, *12*, 959.
(42) Raju, V. R.; Menezes, E. V.; Marin, G.; Graessley, W. W.; Fetters, L. J. *Macromolecules* **1981**, *14*, 1668.
(43) Roovers, J. *Polymer* **1985**, *26*, 1091.
(44) Toporowski, P. M.; Roovers, J. *J. Polym. Sci., Polym. Chem. Ed.* **1986**, *24*, 3009.
(45) Menezes, E. V.; Graessley, W. W. *J. Polym. Sci., Polym. Phys. Ed.* **1982**, *20*, 1817.
(46) Pearson, D. S. *Rubber Chem. Technol.* **1987**, *60*, 439.
(47) Osaki, K.; Takatori, E.; Kurata, M.; Watanabe, H.; Yoshida, H.; Kotaka, T. *Macromolecules* **1990**, *23*, 4392.
(48) Fetters, L. J.; Kiss, A. D.; Pearson, D. S.; Quack, G. F.; Vitus, F. J. *Macromolecules* **1993**, *26*, 647.
(49) Manufacture's designation.
(50) (a) Watanabe, H.; Yamazaki, M.; Yoshida, H.; Adachi, K.; Kotaka, T. *Macromolecules* **1991**, *24*, 5365. (b) Watanabe, H.; Urakawa, O.; Yamada, H.; Yao, M.-L. *Macromolecules*, in press.
(51) Colby, R. H.; Fetters, L. J.; Graessley, W. W. *Macromolecules* **1987**, *20*, 2226.
(52) Doi, M.; Edwards, S. F. *The Theory of Polymer Dynamics*; Clarendon: Oxford, 1986.
(53) Doi, M.; Kuzuu, N. *J. Polym. Sci., Polym. Lett. Ed.* **1980**, *18*, 775.
(54) Pearson, D. S.; Helfand, E. *Macromolecules* **1984**, *17*, 888.
(55) Ball, R. C.; McLeish, T. C. B. *Macromolecules* **1989**, *22*, 1911.
(56) Dimarzio, E. A. *J. Chem. Phys.* **1965**, *42*, 2101.
(57) Hoffmann, M.; Kämpf, G.; Krömer, H.; Pampus, G. *Adv. Chem. Ser.* **1971**, *No. 99*, 351.

MA951249H